PCCP

ROYAL SOCIETY OF CHEMISTRY

PAPER

View Article Online
View Journal | View Issue

Cite this: *Phys. Chem. Chem. Phys.*, 2020, **22**, 5046

Absorption spectra of benzoic acid in water at different pH and in the presence of salts: insights from the integration of experimental data and theoretical cluster models†

Natalia V. Karimova,[a] Man Luo,[b] Vicki H. Grassian[bc] and R. Benny Gerber*[ad]

The absorption spectra of molecular organic chromophores in aqueous media are of considerable importance in environmental chemistry. In this work, the UV-vis spectra of benzoic acid (BA), the simplest aromatic carboxylic acid, in aqueous solutions at varying pH and in the presence of salts are measured experimentally. The solutions of different pH provide insights into the contributions from both the non-dissociated acid molecule and the deprotonated anionic species. The microscopic interpretation of these spectra is then provided by quantum chemical calculations for small cluster models of benzoic species (benzoic acid and benzoate anion) with water molecules. Calculations of the UV-vis absorbance spectra are then carried out for different clusters such as $C_6H_5COOH{\cdot}(H_2O)_n$ and $C_6H_5COO^-{\cdot}(H_2O)_n$, where n = 0–8. The following main conclusions from these calculations and the comparison to experimental results can be made: (i) the small water cluster yields good quantitative agreement with observed solution experiments; (ii) the main peak position is found to be very similar at different levels of theory and is in excellent agreement with the experimental value, however, a weaker feature about 1 eV to lower energy (red shift) of the main peak is correctly reproduced only by using high level of theory, such as Algebraic Diagrammatic Construction (ADC); (iii) dissociation of the BA into ions is found to occur with a minimum of water molecules of n = 8; (iv) the deprotonation of BA has an influence on the computed spectrum and the energetics of the lowest energy electronic transitions; (v) the effect of the water on the spectra is much larger for the deprotonated species than for the non-dissociated acid. It was found that to reproduce experimental spectrum at pH 8.0, additional continuum representation for the extended solvent environment must be included in combination with explicit solvent molecules ($n \geq 3$); (vi) salts (NaCl and $CaCl_2$) have minimal effect on the absorption spectrum and; (vii) experimental results showed that B-band of neutral BA is not sensitive to the solvent effects whereas the effect of the water on the C-band is significant. The water effects blue-shift this band up to ~0.2 eV. Overall, the results demonstrate the ability to further our understanding of the microscopic interpretation of the electronic structure and absorption spectra of BA in aqueous media through calculations restricted to small cluster models.

Received 13th December 2019,
Accepted 10th February 2020

DOI: 10.1039/c9cp06728k

rsc.li/pccp

1. Introduction

Organic acids are widely present in natural waters.[1] These acids can form complexes with transient metals or are components of large complex organic clusters. For example, BA is a simple but important moiety within the large, more complex naturally occurring humic substances found in soils, humic-like substances found in atmospheric aerosols and chromophoric

[a] *Department of Chemistry, University of California, Irvine, CA 92697, USA*
[b] *Department of Chemistry and Biochemistry, University of California, San Diego, CA 92093, USA*
[c] *Department of Nanoengineering and Scripps Institution of Oceanography, University of California, San Diego, CA 92093, USA*
[d] *Institute of Chemistry and Fritz Haber Research Center, Hebrew University of Jerusalem, Jerusalem 91904, Israel. E-mail: benny@fh.huji.ac.il*

† Electronic supplementary information (ESI) available: Proton transfer process between benzoic acid and water molecules: NBOs charges of the fragments $C_6H_5COOH/(C_6H_5COO\cdots H)$ stabilized by 8 water molecules. Theoretical optical absorption spectra of $C_6H_5COOH{\cdot}(H_2O)_8$ *versus* the experimental data at pH 2.5 (theoretical spectrum presented here is an average spectrum of all structures along AIMD trajectories. It shows the effect of the proton transfer on the quality of the theoretical optical spectrum for the system with neutral BA). Table of experimental (in water at pH 2.5) and theoretical spectral data for isolated benzoic acid (different methods and basis sets). Theoretical optical absorption spectra (gas phase) of $C_6H_5COOH{\cdot}(H_2O)_7$ *versus* the experimental data at pH 2.5 (theoretical spectrum presented here is an average spectrum of all structures along AIMD trajectories). Additional data related to this paper can be accessed from the NSF-CAICE Data Repository (https://doi.org/10.6075/J0KS6PZR) or may be requested from the authors. See DOI: 10.1039/c9cp06728k

dissolved organic matter (cDOM) found in the sea surface microlayers and, more recently found within sea spray aerosol.[2–5] All of these are effective photosensitizer,[6,7] exhibit strong absorption extending into the visible spectral region,[8–11] that can play a significant role in the Earth's radiative energy balance. Therefore, systematic investigation of small molecules can provide some initial understanding of the optical properties of these more complex light absorbing substances.

Aromatic organic acids have their own strong absorption bands in the UV range, and are subject to photochemical transformation under solar radiation.[12–15] BA and BA derivatives have three characteristic absorption bands: an A-band around 190 nm (6.5 eV), a B-band around 230 nm (5.5 eV) and a C-band around 280 nm (4.5 eV).[12–14,16] In this paper, we will focus on a study of the 200 to 300 nm region of the optical absorption spectrum (B- and C-bands). There is agreement on several aspects of the absorption spectrum from previous studies including the general shape and position of these bands with the B-band is a strong sharp peak, whereas the C-band is weak and broad.[12–14,16] In addition, the C-band is about 1 eV lower energy from the main B-band. Kamath and co-workers ascribed the B-band to an intramolecular charge transfer or electronic transfer absorption, whereas the C-band was considered as the shifted benzene band.[13] There are some differences in the shape of the curve and the position of the peak maxima for the C-band in polar solvents and alcoholic solutions.[12] Smith *et al.* performed an experimental and made a theoretical study of optical absorption spectra of BA and eight benzoic acid derivatives at different pH in water solutions.[14]

Photoactivation processes of benzoic acid derivatives have also been studied.[17–21] Results show that BA and its derivatives frequently undergo excited state configurational changes such as conformational isomerization,[17] photolysis,[18,19] and proton transfer.[20,21] Nevertheless, investigation of the photoexcitation of BA and BA derivatives is important for further understanding of the processes in larger systems. The photophysical and photochemical properties of these relatively small species in solution are complex, even for single benzoic acid due to: (i) medium effects – many solvent molecules may be involved in influencing the structure and chromophoric activity[22] and; (ii) contribution of the speciated forms (neutral molecules and their deprotonated anions) to the optical absorption spectrum can be significant. An important source of information is pH, which changes the equilibrium between neutral and anionic species.[23,24] In such cases, the combination of the experimental study with theoretical simulations can provide deeper insight into processes of photoactivation of molecules, for example, benzoic acid.

In this work, experimental spectroscopic measurements are combined with theoretical calculations to study the optical absorption spectra of BA in aqueous solution at different pH, which therefore throws the light both on the non-dissociated molecule and on the anionic speciated form of BA. Experimental measurements were performed for BA with concentration 0.1 mM in the solution of water, 0.5 M NaCl and 0.167 M $CaCl_2$. As benzoic acid has two speciated forms, the UV-vis experiments are carried out at pH = 2.5 and pH = 8.0 which correspond to the two different species: protonated and deprotonated forms, respectively (pHs are adjusted using 1 N HCl and 1 N NaOH). Theoretical calculations were performed for several small clusters of the formulae $C_6H_5COOH{\cdot}(H_2O)_n$ and $C_6H_5COO^-{\cdot}(H_2O)_n$ (where n = 0–8) in gas phase and with additional the extended solvent environment (polarizable continuum model). *Ab initio* Molecular Dynamic simulations in the ground state were performed to include all possible speciated forms into the total optical absorption spectrum. To calculate the excitation energies and oscillator strength, methods ADC(n) (where n = 2 and 3)[25,26] and TDDFT[27] were applied. Additionally, solvent effects on the simulated optical absorption spectra of neutral and ionized speciated forms of BA were studied. Solvent effects were included using two approaches. The first involves only explicit water molecules were introduced into our model systems (calculations were performed in gas phase). The second where explicit water molecules are combined with continuum representation for the extended solvent environment (isolated and hydrated BA clusters were calculated using polarizable continuum model). This systematic investigation of the photoexcitation of BA is very important for further understanding of more complex organic substances.

Additionally, we want to state main achievements of this study. Introduction of the high level of theory such ADC allowed to obtain additional information about systems of interest. Specifically, we were confirmed with appropriate interpretation of the weak low-energy peak (C-band). Investigation of strength and limitations of cluster model for simulation of BA in solution at different pH were obtained. Now we understand the relationships between cluster model and continuum model.

2. Experimental data

The UV-vis spectra between 200 nm to 300 nm for benzoic acid in water at acidic and basic pH is shown in Fig. 1a. Based on the pK_a of 4.2 for benzoic acid,[28] the absorption spectrum at pH 2.5 represent that for neutral benzoic acid as the system consists above 98% of neutral species at this pH and the absorption spectrum at pH 8 represent that for anion species as the system consists above 99.9% of anionic species at pH 8. The neutral benzoic acid at acidic pH obtain higher absorbance and red shift on both B-band and C-band compare to anion species. The B-band peak maximum for neutral and anion species were found to be centered at 230 nm and 225 nm respectively. The C-band is broad with the peak maximum centered at around 274 nm and 269 nm for neutral and anion species, respectively. These results are in agreement with previous studies.[14,16] The effect of salt ions that commonly found in the marine environment, such as NaCl and $CaCl_2$, on the absorption spectra of benzoic acid were also tested, which is shown in Fig. 1b and c. No obvious difference observed between the spectra for benzoic acid in water and in other salt solutions at both acidic and slightly basic pH.

3. Theoretical methods and models

Theoretical calculations were performed for a neutral molecule of benzoic acid and its anion in the gas phase and stabilized by

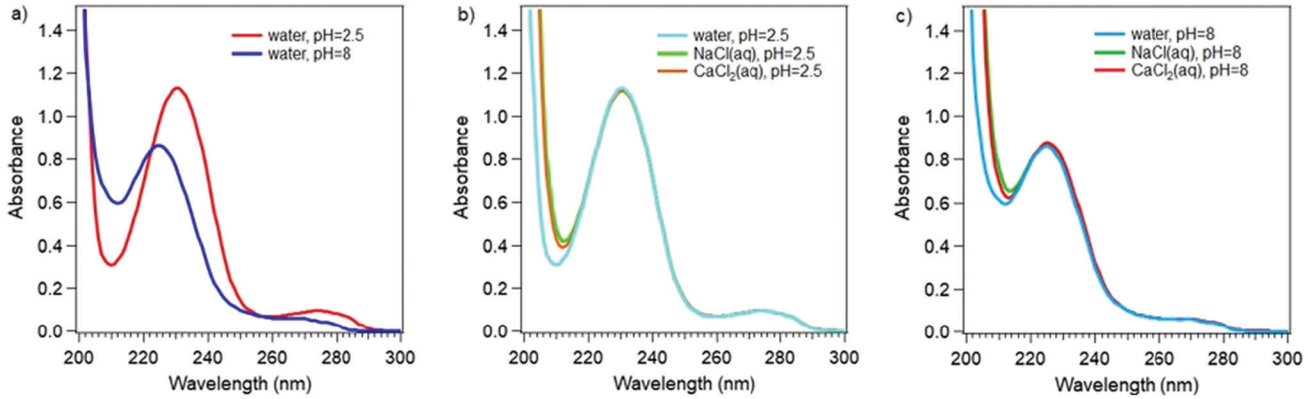

Fig. 1 Experimental UV-vis spectra of 0.1 mM benzoic acid in aqueous solutions: (a) in water at pH 2.5 and 8; (b) in water compared to in 0.5 M NaCl and 0.167 M $CaCl_2$ solutions at pH 2.5; and (c) in water compared to in 0.5 M NaCl and 0.167 M $CaCl_2$ solutions at pH 8.0.

water molecules. All calculations were performed using Q-Chem program.[29] Geometry optimizations employ the B3LYP functional[30] and basis set 6-31+G*. Additionally, for hydrated species, dispersion corrections from Grimme's DFT-D2 method were used.[31]

Models for BA at pH 2.5.

It was mentioned that at pH 2.5 the system consists above 98% of neutral species of BA. Recent theoretical study[32] showing that proton transfer from a neutral benzoic acid molecule to solvent water molecules occurs only when at least eight water molecules are attached to the benzoic acid, forming a hydrated cluster. Our AIMD calculations for $C_6H_5COOH{\cdot}(H_2O)_8$ cluster also detected the proton transfer from neutral BA to the water cluster (and *vice versa*):

$$C_6H_5COOH{\cdot}(H_2O)_8 \rightleftarrows C_6H_5COO^{-}{\cdot}(H_3O)^{+}{\cdot}(H_2O)_7$$

Partial charge analysis along the AIMD trajectories showed that half of the time BA exists in a neutral form $C_6H_5COOH{\cdot}(H_2O)_8$ and another half of the time it is ionized as $C_6H_5COO^{-}{\cdot}H_3O^{+}{\cdot}(H_2O)_7$ (Fig. S1, ESI†). This ionization process plays a significant influence on the quality of the final optical absorption spectrum (Fig. S2, ESI†).

Therefore, to avoid the proton transfer in our model the only clusters of BA with up to 7 water molecules will be considered ($C_6H_5COOH{\cdot}(H_2O)_n$ where n = 0–7). The initial ground state geometries of these clusters were implemented from the theoretical study.[32]

Models for BA at pH 8.0

This system consists above 99.9% of anionic species ($C_6H_5COO^{-}$) at this pH. For this system, the proton transfer issue was not detected for systems even with 8 water molecules. Thus, for simulation of the optical spectrum at current pH, model systems $C_6H_5COO^{-}{\cdot}(H_2O)_n$ (where n = 0–8) were considered. The initial ground state geometries of these clusters were obtained by removing the proton from BA in the neutral clusters $C_6H_5COOH{\cdot}(H_2O)_n$.

Optical absorption spectra

Excitation spectra are calculated using the Time-dependent Density Functional Theory (TDDFT)[27] method such as B3LYP[33,34] which was assessed with standard People (6-31+G*, 6-311+G*, 6-311++G**) and Dunning (aug-cc-pVTZ and aug-cc-PVQZ) basis sets.[35,36] High-level calculations such as the Algebraic Diagrammatic Construction (ADC)[26,37,38] were performed as the benchmark TDDFT. Shemesch *et al.*[38] demonstrated that ADC level of theory can be successfully applied for study of photoinduced reactions of carboxylic acids, such as acrylic acid. The ADC(3) and ADC(2) methods with 6-31+G*, 6-311+G*, 6-311++G** basis sets were applied for simulation of the optical absorption spectrum of the global minimum of the isolated BA molecule.

Only a moderate basis set effect was found for all considered methods (the maximum difference in the position of the peaks is ~0.04 eV). However, the closest results to aug-cc-pVQZ basis set obtained using aug-cc-pVTZ and 6-311++G**. The basis sets assessment is given in the ESI† (Table S1). Therefore, the 6-311++G** basis set was chosen for further calculations, including the molecular orbital analysis and UV spectra calculations.

All presented in the current work experimental spectra were obtained in water solution. Thus, it is very important to take solvent effects into account for calculations of the UV spectra. To do this, the explicit solvent molecules (water clusters in our suggested models) were combined with the polarizable continuum model (C-PCM).[39] The C-PCM was employed in combination with B3LYP/6-311++G** method. Solute cavities are constructed from a union of atom-centered spheres whose radii are 1.2 times the atomic van der Waals radii suggested by Bondi.[40]

To describe the nature of the excited states, the hole/particle Natural Transition Orbitals (NTOs)[41,42] pairs were calculated for every excited state involved into formation of B- and C-bands.

AIMD simulations

To include all possible speciated forms into the total optical spectrum the combinations of AIMD with TDDFT was suggested. To explore this, we applied *ab initio* molecular dynamics (AIMD)[43,44] method for systems $C_6H_5COOH{\cdot}(H_2O)_7$ and $C_6H_5COO^{-}{\cdot}(H_2O)_8$ at constant energy in the ground state, with potentials at the B3LYP/6-31+G* level of theory. Initial velocities were sampled for the equilibrium structure of interest from a Boltzmann distribution at 298 K. A total of 10 reactive trajectories per system were propagated for up to 7.0 ps using a time-step of 0.4 fs. From

each trajectory, we extracted a structure every 40 fs of the simulation, and their vertical excitation energies and oscillator strengths were calculated with the B3LYP/6-311++G** (with C-PCM). For each excitation energy, the vertical transitions were convoluted with a Lorentzian line shape with a width of 20 nm, and all of the resulting Lorentzians were added to yield the excitation spectrum. This approach was previously used by Shemesh and co-workers[45] for simulation of β-hydroxyalkyl nitrates.

4. Results and discussion

Spectra of isolated benzoic acid species

Theoretical optical absorption spectrum (in gas phase) of neutral BA calculated with B3LYP/6-311++G**, ADC(2)/6-311++G** and ADC(3)/6-311++G** is compared with experimental spectrum in water at acidic pH of 2.5 (Table 1 and Fig. 2).

Experimental results showed that B-band of neutral BA is not sensitive to the solvent effects (Table 1). Both optical spectra of isolated BA[46] and BA in water at pH 2.5 exhibit B-band at 5.4 eV (230 nm). However, the effect of the water on the C-band is significant. The C-band of isolated BA[46] appears between 4.59–4.68 eV (265–270 nm), whereas the water effects blue-shift this band up to ~0.2 eV (Table 1). The maximum energy gap between experimental B- and C-bands are around 0.8 and 1 eV for isolated BA and for BA in water at pH 2.5, respectively.

All considered theoretical methods exhibit both absorption bands (B- and C-) for benzoic acid in the range of 200–300 nm (Table 1 and Fig. 2). As shown in Fig. 2a and b, offsetting the theoretically predicted peaks by 0.2 eV (~12 nm) for ADC(3) and 0.45 eV (17 nm) for ADC(2) methods leads to a very good agreement with the experimental data. It is important to mention, that the energy gap between theoretical B- and C-bands is between 0.9–1 eV (both ADC methods), which is in good agreement with the experiment (Table 1).

TDDFT (B3LYP/6-311++G**) optical absorption spectrum of isolated benzoic acid showed that the theoretical B-band has the exact position as in the experiment and is localized around 231 nm (5.36 eV) (Fig. 2c and Table 1). The C-band is significantly blue shifted with respect to experiment: the energy difference between B- and C-bands is around 0.51 eV only (which is smaller by ~0.3 eV than the experimental value for isolated BA[46]). Smith and co-worker,[14] calculated optical absorption spectrum of neutral BA using different exchange–correlation (XC) functionals such as meta-GGA hybrid M06-2X, double hybrid B2PLYPD,

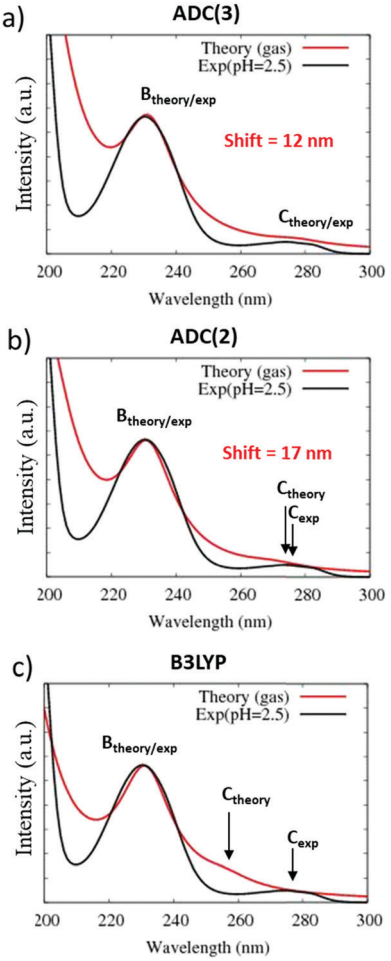

Fig. 2 Comparison of the optical spectrum of isolated molecule C_6H_5COOH obtained using ADC(3), ADC(2) and B3LYP methods (basis set is 6-311++G**) with experimental data at pH 2.5: (a) theory ADC(3) *vs.* experiment pH 2.5; (b) theory ADC(2) *vs.* experiment pH 2.5; and (c) theory B3LYP *vs.* experiment at pH 2.5.

and range-separated functionals CAM-B3LYP, ωB97XD, and LC-ωPBE, but all tested functionals could not reproduce the correct energy gap between B- and C-bands as well.

Additionally, the hole/particle NTO pairs were calculated for the first three excited states for all three methods. The energy of these excited states, their oscillator strength and NTOs pairs are present in Fig. 3. According to the method ADC(3), the low-lying excitations (C-band) occurs due to $\pi \rightarrow \pi^*$ electron transition only, whereas the strong and sharp B-band is a mixture of both

Table 1 Experimental (in water at pH 2.5), experimental and theoretical optical absorption spectral data for benzoic acid (where the $\Delta(E_B - E_C)$ is the energy gap between the maximums of C- and B-bands)

	Peak maximum		
Method	C-band	B-band	$\Delta(E_B - E_C)$
Experiment in water (pH 2.5)	4.35–4.50 eV (275–285 nm)	5.40 eV (230 nm)	0.90–1.05 eV
Experiment isolated BA[46]	4.59–4.68 eV (265–270 nm)	5.40 eV (230 nm)	0.72–0.81 eV
ADC(3)/6-311++G**	4.70 eV (264 nm)	5.69 eV (218 nm)	0.99 eV
ADC(2)/6-311++G**	4.95 eV (250 nm)	5.84 eV (213 nm)	0.89 eV
B3LYP/6-311++G**	4.85 eV (256 nm)	5.36 eV (231 nm)	0.51 eV

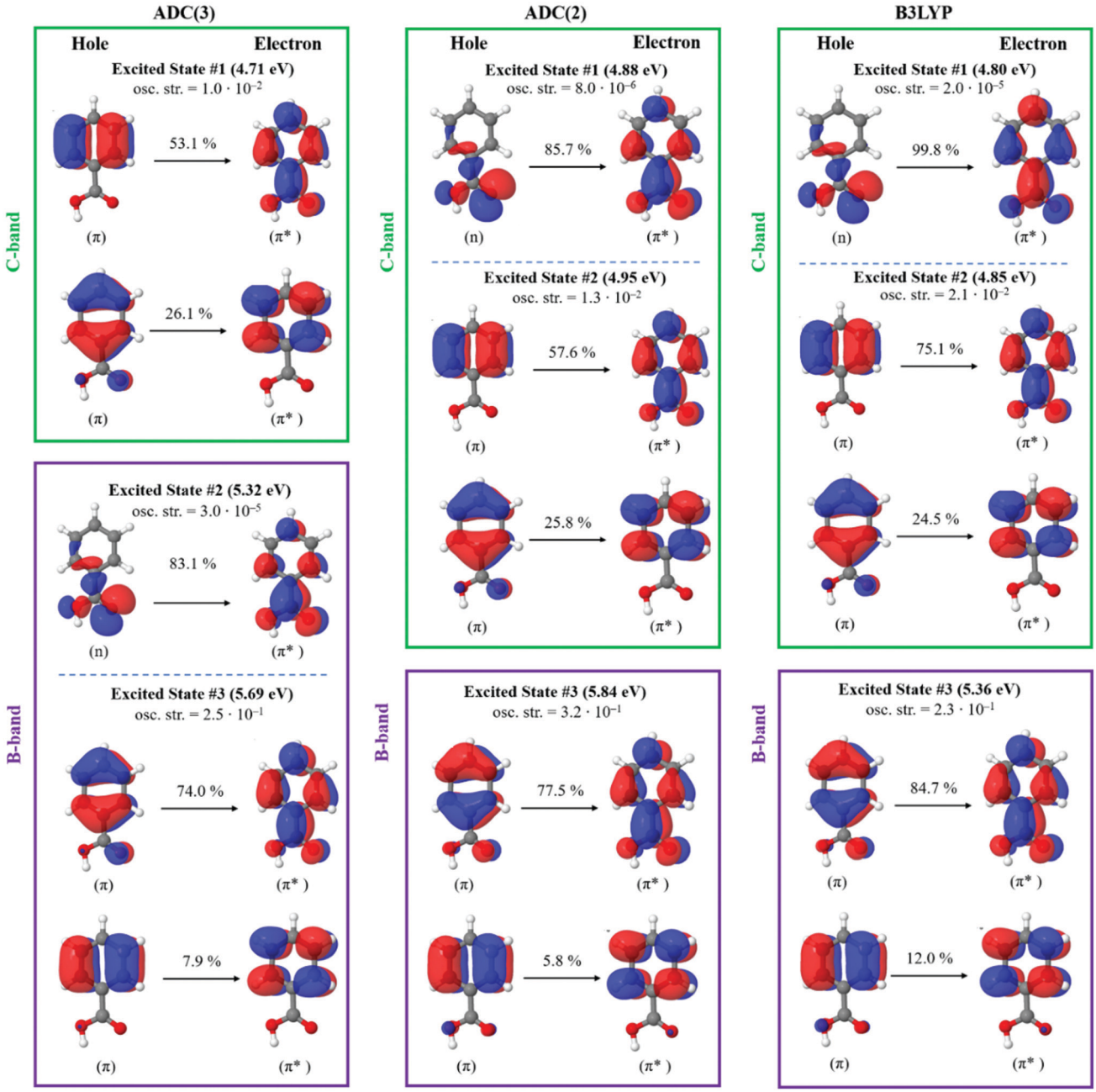

Fig. 3 Natural transition orbitals of the first three excited states (formed B and C-bands) of BA molecule calculated at the ADC(3), ADC(2) and B3LYP level of theory with basis set 6-311++G**. Orbitals are represented with a contour value of 0.035.

transitions: n $\rightarrow\pi^*$ and $\pi \rightarrow \pi^*$ (Fig. 3). Nevertheless, methods ADC(2) and B3LYP exhibits the opposite results: C-band is a mixture of n $\rightarrow\pi^*$ and $\pi \rightarrow \pi^*$ electron transitions, and the B-band arises due to $\pi \rightarrow \pi^*$ electron transition only. It should be noticed, that in all methods, the oscillator strength of the excited states which assign with n $\rightarrow\pi^*$ transitions are very weak (amplitudes are 10^{-5}–10^{-6}) (Fig. 3). Therefore, we can expect that contributions to the formation of the B-and C-bands of neutral BA are mainly from $\pi \rightarrow \pi^*$ electron transitions.

These theoretical results allowed us to conclude that, TDDFT reproduces correctly the shape and maximum position of the strong B-band (good agreement with experiment). However, in the case of C-band, TDDFT cannot reproduce the correct position of this band (it is blue-shifted by ~0.3–0.4 eV with respect to experimental C-band), but TDDFT reproduces the nature of involved orbitals with ADC(2) level accuracy. In addition, TDDFT is computationally less expensive with respect to ADC(n) levels of theory. Thus, in this work, TDDFT level of theory will be used to study the nature of B-band only.

Cluster size and predicted spectra: $C_6H_5COOH{\cdot}(H_2O)_n$ and $C_6H_5COO^-{\cdot}(H_2O)_n$ (n = 0–8)

To check the effect of the solvent effects on the optical properties of the BA at different pH two speciated forms of BA stabilized by

water cluster of different sizes were tested: $C_6H_5COOH\cdot(H_2O)_n$ and $C_6H_5COO^-\cdot(H_2O)_n$ (n = 0–8). Optical absorption spectra of these clusters were calculated using B3LYP/6-311++G** method in the gas phase and with the additional inclusion of a continuum representation for the extended solvent environment (C-PCM).

Benzoic acid with water molecules ($C_6H_5COOH\cdot(H_2O)_n$)

The isolated neutral molecule of BA and BA hydrated clusters were used for simulations of the experimental spectrum of BA at low pH = 2.5. The ground state minimum energy equilibrium structures $C_6H_5COOH\cdot(H_2O)_n$ (n = 0–7) and their optical spectra are shown in Fig. 4. Theoretical results demonstrated that the shape of the optical spectrum of neutral BA form is not significantly sensitive to the number of water molecules in the considered clusters. Results obtained in the gas phase calculations (red curve) showed that all considered systems exhibit the B-band around 230 nm (excellent agreement with experiment). The maximum shift of theoretical B-band (around 0.1 eV (5 nm)) obtained for the larges system $C_6H_5COOH\cdot(H_2O)_7$. However, note, that this cluster is just one possible structure of the system and when we consider the contribution to the total optical absorption spectrum of all structures from MD trajectories, the position of theoretical B-band can be improved.

The additional solvent effects such as the polarizable continuum model (C-PCM) does not make any significant changes in the shape of the optical spectra of these neutral clusters. However, the B-band is red-shifted with respect to the experiment by 0.2 eV (~10 nm). The reason for this shift can be the interaction of the hydrophobic Ph-group with the continuum.

Benzoate anion with water molecules ($C_6H_5COO^-\cdot(H_2O)_n$)

To simulate the experimental spectrum of BA at high pH = 8.0, the ionized form of BA was considered with different number of water molecules $C_6H_5COO^-\cdot(H_2O)_n$ (n = 0–8). The experimental B-band of this system arises around 225 nm. The obtained results showed that the spectrum of $C_6H_5COO^-$ is significantly sensitive to solvent effects (Fig. 5). For example, the theoretical optical absorption spectrum of isolated $C_6H_5COO^-$ does not

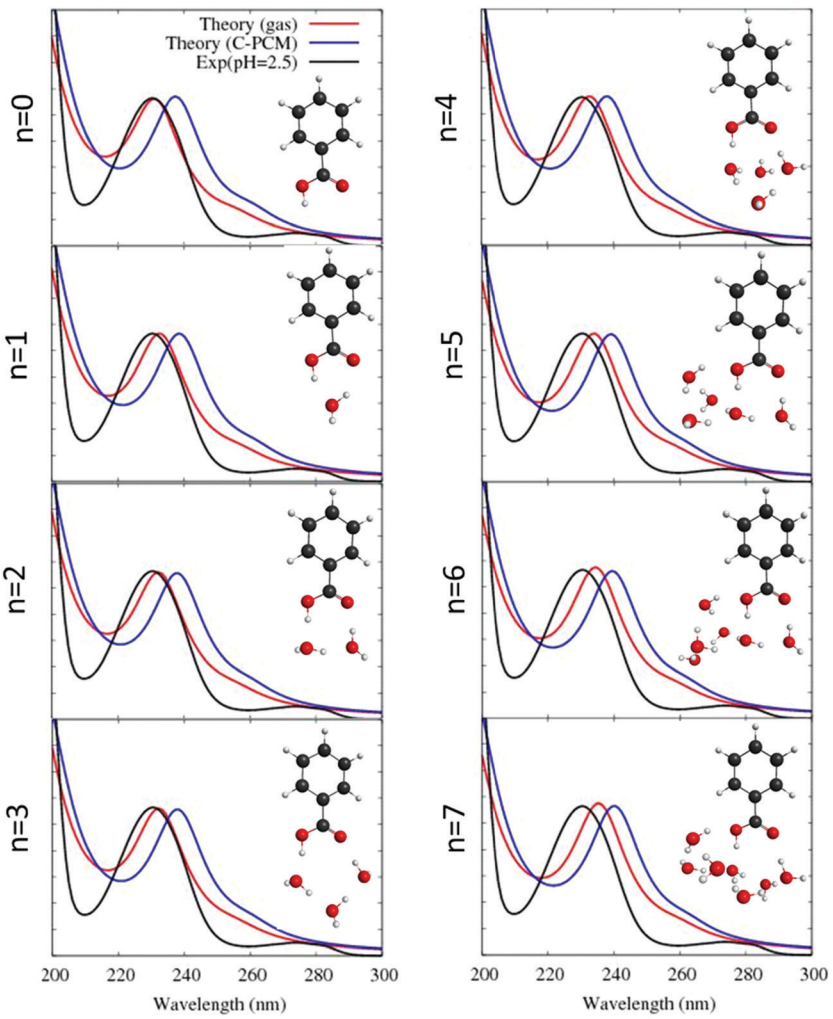

Fig. 4 Experimental optical absorption spectrum at pH 2.5 (black line), theoretical optical absorption spectra of neutral clusters (equilibrium structures) $C_6H_5COOH\cdot(H_2O)_n$ (where n = 0–7) in gas phase (red line) and with including solvent effects (C-PCM) (blue line). Level of theory is B3LYP/6-311++G**.

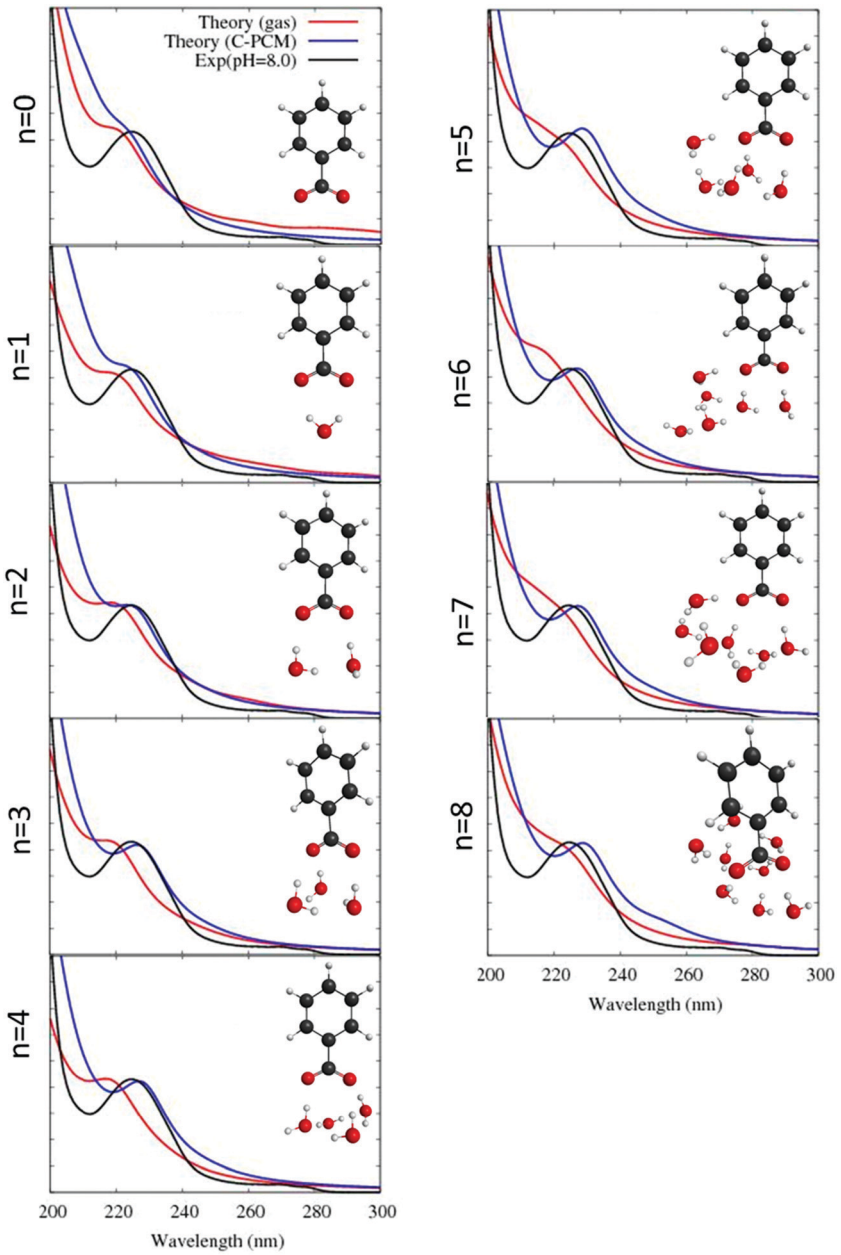

Fig. 5 Experimental optical absorption spectrum at pH 8.0 (black line), theoretical optical absorption spectra of ionized clusters (equilibrium structures) $C_6H_5COO^-(H_2O)_n$ (where n = 0–8) in gas phase (red line) and with including solvent effects (C-PCM) (blue line). Level of theory is B3LYP/6-311++G**.

exhibit any peaks between 200–300 nm (Fig. 5). Stabilization of the BA anion with one water molecules allowed us to localize one shoulder peak around 218 nm (Fig. 5) in gas phase.

Significant improvements with the position of the B-band maximum and the curve shape were obtained when a model system with $n \geq 3$ water molecules was considered and additional internal solvent effects were included (CPCM). For example, the largest system $C_6H_5COO^-\cdot(H_2O)_8$ exhibit the sharp peak around 5.41 eV (229 nm), the difference with experiment is just 4 nm now (Fig. 5).

Comparison spectra of neutral and ionized BA forms

To understand the difference between the optical properties of BA at different pH (two speciated forms), the optical absorption spectra of two largest clusters (equilibrium structures) $C_6H_5COOH\cdot(H_2O)_7$ and $C_6H_5COO^-(H_2O)_8$ were compared. The theoretical optical absorption spectra together with the oscillator strength of the excited states for $C_6H_5COOH\cdot(H_2O)_7$ and $C_6H_5COO^-(H_2O)_8$ clusters are presented in Fig. 6 (method is B3LYP/6-311++G** with including C-PCM algorithm). In the cluster $C_6H_5COOH\cdot(H_2O)_7$, the B-band arises due to one strong excited state at 5.16 eV (240 nm, f = 0.370), Fig. 6a. In the case of $C_6H_5COO^-\cdot(H_2O)_8$, the B-band has a maximum at 5.39 eV (229 nm) and it is more complex with respect to neutral BA cluster: it is formed by two excited states at 5.12 eV (242 nm, f = 0.0014) and 5.39 eV (229 nm, f = 0.230), Fig. 6b.

The NTOs pairs involved in the transitions of the B-band both clusters are shown in Fig. 7. The orbitals have similar

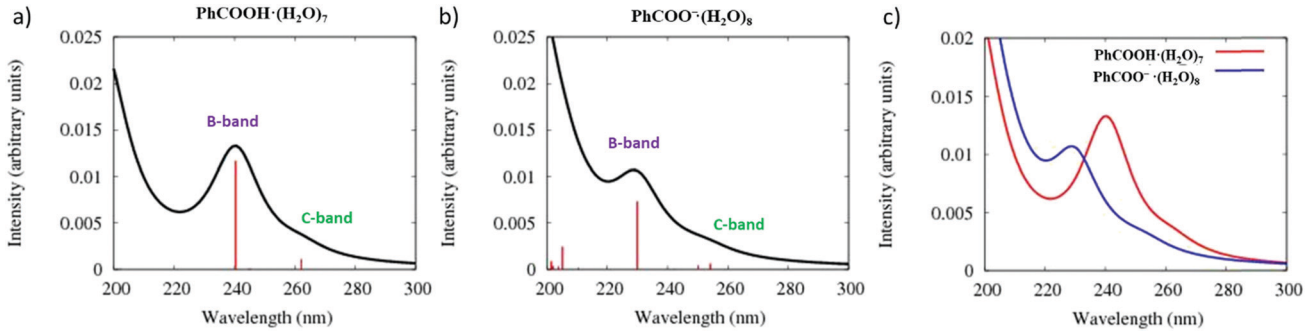

Fig. 6 Theoretical optical absorption spectra calculated using B3LYP/6-311++G** with including solvent effects (C-PCM): (a) of neutral cluster $C_6H_5COOH{\cdot}(H_2O)_7$; (b) clusters $C_6H_5COO^-$ $(H_2O)_8$; and (c) comparison these two theoretical spectra.

features but there are subtle differences as well. For example, in the optical absorption spectrum of $C_6H_5COOH{\cdot}(H_2O)_7$ system, the B-band arises due to $\pi \rightarrow \pi^*$ only (Fig. 7a). However, in the cluster $C_6H_5COO^-{\cdot}(H_2O)_8$, non-bonding HOMO orbitals are involved as well: $n \rightarrow \pi^*$ and $\pi \rightarrow \pi^*$ transitions (Fig. 7b). Comparison of the orbitals of $C_6H_5COOH{\cdot}(H_2O)_7$ cluster with orbitals of the isolated C_6H_5COOH molecule in the gas phase showed, that in both cases the orbitals involved in the electron transitions of the B-band localized on the BA fragment (Fig. 3 and 7a).

Additionally, obtained theoretical data reproduce the relative intensities of B-band at different pH (Fig. 1a and 6c). Experimental B-band at pH 2.5 ($I_{exp(2.5)}$) much intense than at pH 8.0 ($I_{exp(8.0)}$). The ratio of experimental B-band intensities is $\frac{I_{exp(8.0)}}{I_{exp(2.5)}} = 0.76$. Theoretical ratio of B-band intensities for considered clusters is very close to the experimental value and equivalent to $\frac{I_{PhCOO^-{\cdot}(H_2O)_8}}{I_{PhCOOH{\cdot}(H_2O)_7}} = 0.80$.

AIMD simulations and final optical spectra of $C_6H_5COOH{\cdot}(H_2O)_7$ and $C_6H_5COO^-{\cdot}(H_2O)_8$

To consider the contribution to the total optical absorption spectrum of all possible structures, AIMD trajectories were simulated and used to calculate total TDDFT optical absorption spectrum of largest systems: $C_6H_5COOH{\cdot}(H_2O)_7$ and $C_6H_5COO^-{\cdot}(H_2O)_8$. It was found (Fig. 4 and 5) that in the case of $C_6H_5COO^-$ that additional explicit solvent molecules are needed to be included in combination with a continuum representation for the extended solvent environment to be able to reproduce the experimental spectrum correctly. Method for calculation of vertical excited states along AIMD trajectories is B3LYP/6-311++G** with including additional solvent effects by C-PCM.

Overall, the total theoretical optical absorption spectra of $C_6H_5COOH{\cdot}(H_2O)_7$ and $C_6H_5COO^-{\cdot}(H_2O)_8$ systems from the AIMD simulations are presented in Fig. 8. The maximum of the B-band was found at 5.16 eV (240 nm) for $C_6H_5COOH{\cdot}(H_2O)_7$ and 5.41 eV (229 nm) for $C_6H_5COO^-{\cdot}(H_2O)_8$. As shown in Fig. 8a and b, offsetting the theoretically predicted peaks by 4

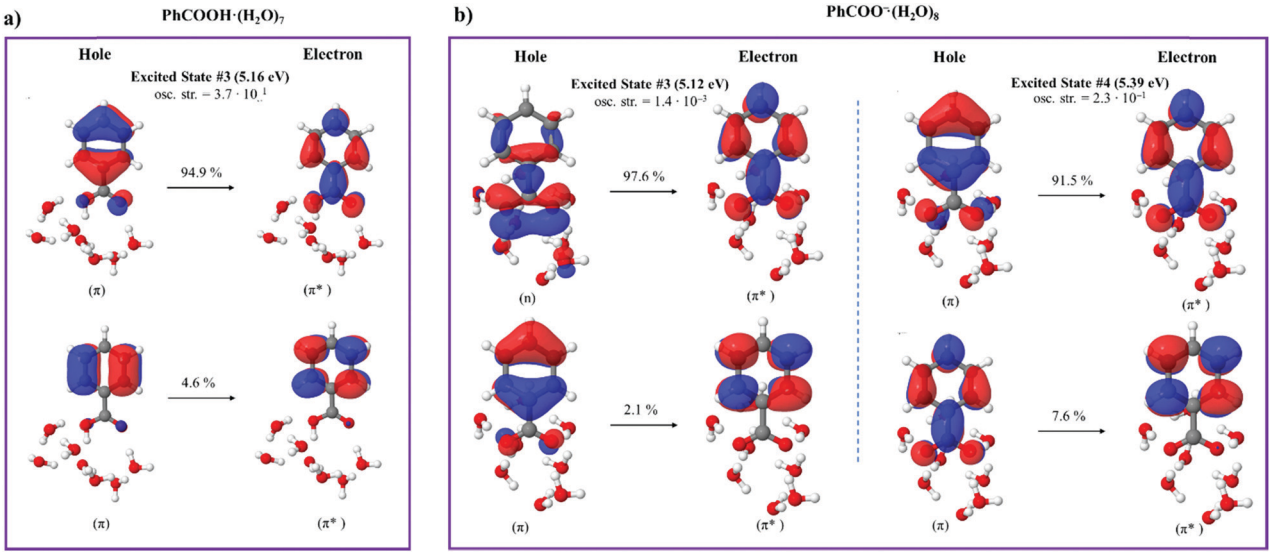

Fig. 7 Natural transition orbitals of the excited states (for B-band) of two speciated forms of BA: (a) $C_6H_5COOH{\cdot}(H_2O)_7$ and (b) $C_6H_5COO^-$ $(H_2O)_8$ calculated at the B3LYP/6-311++G** (with including solvent effects by C-PCM). Orbitals are represented with a contour value of 0.035.

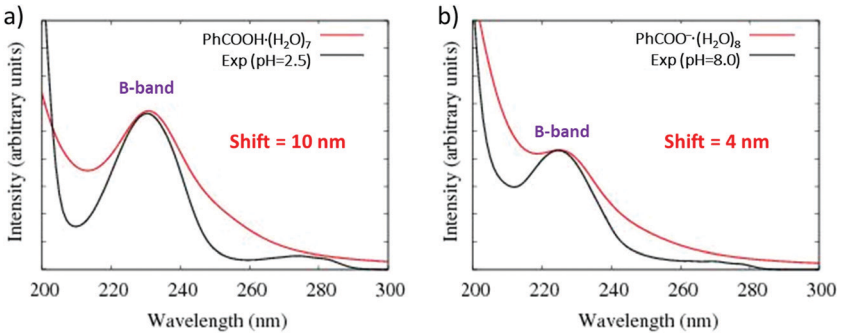

Fig. 8 Comparison of the theoretical and experimental spectral data. Theoretical spectrum presented here is an average spectrum of all structures along AIMD trajectories. Optical absorption spectra of (a) $C_6H_5COOH\cdot(H_2O)_7$ *versus* the experimental data at pH 2.5; and (b) $C_6H_5COO^-\cdot(H_2O)_8$ *versus* the experimental data at pH = 8.0. Method B3LYP/6-311++G** (with including solvent effects by C-PCM). Theory – red curve, experiment – black.

(for ionized BA) and 10 (neutral BA) nm leads to a very good agreement with the experimental data. In the case of the neutral structure $C_6H_5COOH\cdot(H_2O)_7$, the 10 nm shift is related to the effect of the extended solvent environment model (C-PCM). Additional calculations of total (AIMD) optical absorption spectrum for $C_6H_5COOH\cdot(H_2O)_7$ in the gas phase allowed us to localize B-band at 234 nm (experimental value is 230 nm), Fig. S3 (ESI†).

5. Concluding remarks

In the present work, experimental spectroscopic measurements are combined with theoretical calculations to study the optical absorption spectra of BA in aqueous solution at different pH. The experimental results for absorption spectra of benzoic acid in water at acidic and basic pH are in agreement with early studies. There is no obvious effect on the benzoic acid absorption spectra found due to the presence of salt ions such as NaCl and $CaCl_2$. Experimental results showed that B-band of neutral BA is not sensitive to the solvent effects whereas the effect of the water on the C-band is significant.[46] The water effects blue-shift this band up to ~0.2 eV.

Small theoretical clusters of BA with different numbers of water molecules demonstrated that solvent effects are very important for reproducing the correct optical spectra of BA species: especially for the deprotonated form of BA such as $C_6H_5COO^-\cdot(H_2O)_n$ (where n = 0–8). Only systems with $n \geq 3$ water molecules combined with the extended solvent environment provide a good agreement with the experiment, in particular, the shape and the maximum position of the B-band.

Small theoretical clusters can be successful in describing chromophores in solution. Theoretical results showed that B-band of neutral BA (experiment at pH 2.5) arises from the $\pi \rightarrow \pi^*$ transitions only, whereas in the case of ionized BA (experiment at pH 8.0) this band appears due to the combination of $n \rightarrow \pi^*$ and $\pi \rightarrow \pi^*$ transitions. NTOs analysis of the theoretical clusters allowed us to see that the orbitals involved in the electron transitions of the B-band are mainly localized on the BA molecule, which indicates that the excitations have a contribution from BA and ion of BA.

Overall, we can conclude that the combination of the excited states quantum chemistry with molecular dynamics provides a very good interpretation of the experiment, and the results demonstrate the possibility of microscopic understanding of the absorption spectra of organic molecules in water by calculations restricted to small cluster models.

Author contributions

Natalia V. Karimova performed theoretical simulations; Man Luo made experimental measurements. Vicki H. Grassian (experimental aspects) and R. Benny Gerber (theoretical aspects) participated in the analysis of results and conclusions and are corresponding authors.

Conflicts of interest

There are no conflicts to declare.

Acknowledgements

The authors would like to gratefully acknowledge supported by the National Science Foundation through the Center for Aerosol Impacts on Chemistry of the Environment funded under the Centers for Chemical Innovation Program Grant CHE1801971. Additionally, this work used the Extreme Science and Engineering Discovery Environment (XSEDE),[47] which is supported by grand number grant number TG-CHE170064. The authors would also like to thank Professor Juan Navea and Dr Dorit Shemesh for helpful discussions.

References

1 E. M. Thurman, *Organic Geochemistry of Natural Waters*, Springer, Netherlands, Dordrecht, 1985.
2 W. S. Wan Ngah, M. A. K. M. Hanafiah and S. S. Yong, Adsorption of humic acid from aqueous solutions on cross-linked chitosan–epichlorohydrin beads: kinetics and isotherm studies, *Colloids Surf., B*, 2008, **65**, 18–24.
3 D. Kwon, M. J. Sovers, V. H. Grassian, P. D. Kleiber and M. A. Young, Optical Properties of Humic Material Standards: Solution Phase and Aerosol Measurements, *ACS Earth Space Chem.*, 2018, **2**, 1102–1111.

4 F. Nasser and I. Lynch, Secreted protein eco-corona mediates uptake and impacts of polystyrene nanoparticles on Daphnia magna, *J. Proteomics*, 2016, **137**, 45–51.
5 S. Jayalath, H. Wu, S. C. Larsen and V. H. Grassian, Surface Adsorption of Suwannee River Humic Acid on TiO_2 Nanoparticles: A Study of pH and Particle Size, *Langmuir*, 2018, **34**, 3136–3145.
6 J. V. Trueblood, M. R. Alves, D. Power, M. V. Santander, R. E. Cochran, K. A. Prather and V. H. Grassian, Shedding Light on Photosensitized Reactions within Marine-Relevant Organic Thin Films, *ACS Earth Space Chem.*, 2019, **3**, 1614–1623.
7 K. McNeill and S. Canonica, Triplet state dissolved organic matter in aquatic photochemistry: reaction mechanisms, substrate scope, and photophysical properties, *Environ. Sci.: Processes Impacts*, 2016, **18**, 1381–1399.
8 C. Baduel, D. Voisin and J.-L. Jaffrezo, Seasonal variations of concentrations and optical properties of water soluble HULIS collected in urban environments, *Atmos. Chem. Phys.*, 2010, **10**, 4085–4095.
9 A. Hoffer, A. Gelencsér, P. Guyon, G. Kiss, O. Schmid, G. P. Frank, P. Artaxo and M. O. Andreae, Optical properties of humic-like substances (HULIS) in biomass-burning aerosols, *Atmos. Chem. Phys.*, 2006, **6**, 3563–3570.
10 Y.-P. Chin, G. Aiken and E. O'Loughlin, Molecular Weight, Polydispersity, and Spectroscopic Properties of Aquatic Humic Substances, *Environ. Sci. Technol.*, 1994, **28**, 1853–1858.
11 D. P. Veghte, S. China, J. Weis, L. Kovarik, M. K. Gilles and A. Laskin, Optical Properties of Airborne Soil Organic Particles, *ACS Earth Space Chem.*, 2017, **1**, 511–521.
12 H. E. Ungnade and R. W. Lamb, The Absorption Spectra of Benzoic Acid and Esters, *J. Am. Chem. Soc.*, 1952, **74**, 3789–3794.
13 B. V. Kamath, J. D. Mehta and S. L. Bafna, Ultraviolet absorption spectra: Some substituted benzoic acids, *J. Appl. Chem. Biotechnol.*, 2007, **25**, 743–751.
14 H.-B. Guo, F. He, B. Gu, L. Liang and J. C. Smith, Time-Dependent Density Functional Theory Assessment of UV Absorption of Benzoic Acid Derivatives, *J. Phys. Chem. A*, 2012, **116**, 11870–11879.
15 M. Karabacak, Z. Cinar, M. Kurt, S. Sudha and N. Sundaraganesan, FT-IR, FT-Raman, NMR and UV-vis spectra, vibrational assignments and DFT calculations of 4-butyl benzoic acid, *Spectrochim. Acta, Part A*, 2012, **85**, 179–189.
16 C. E. Lund Myhre and C. J. Nielsen, Optical properties in the UV and visible spectral region of organic acids relevant to tropospheric aerosols, *Atmos. Chem. Phys.*, 2004, **4**, 1759–1769.
17 S. Amiri, H. P. Reisenauer and P. R. Schreiner, Electronic Effects on Atom Tunneling: Conformational Isomerization of Monomeric *Para*-Substituted Benzoic Acid Derivatives, *J. Am. Chem. Soc.*, 2010, **132**, 15902–15904.
18 I. P. Pozdnyakov, V. F. Plyusnin and V. P. Grivin, Photophysics and Photochemistry of 2-Aminobenzoic Acid Anion in Aqueous Solution, *J. Phys. Chem. A*, 2009, **113**, 14109–14114.
19 A. L. Sobolewski and W. Domcke, Photophysics of intramolecularly hydrogen-bonded aromatic systems: ab initio exploration of the excited-state deactivation mechanisms of salicylic acid, *Phys. Chem. Chem. Phys.*, 2006, **8**, 3410.
20 D. M. Friedrich, Z. Wang, A. G. Joly, K. A. Peterson and P. R. Callis, Ground-State Proton-Transfer Tautomer of the Salicylate Anion, *J. Phys. Chem. A*, 1999, **103**, 9644–9653.
21 D. Vulpius, G. Geipel and G. Bernhard, Excited-state proton transfer of 3-hydroxybenzoic acid and 4-hydroxybenzoic acid, *Spectrochim. Acta, Part A*, 2010, **75**, 558–562.
22 M. C. Almandoz, M. I. Sancho and S. E. Blanco, Spectroscopic and DFT study of solvent effects on the electronic absorption spectra of sulfamethoxazole in neat and binary solvent mixtures, *Spectrochim. Acta, Part A*, 2014, **118**, 112–119.
23 P. C. Mowery, R. H. Lozier, Q. Chae, Y.-W. Tseng, M. Taylor and W. Stoeckenius, Effect of acid pH on the absorption spectra and photoreactions of bacteriorhodopsin, *Biochemistry*, 1979, **18**, 4100–4107.
24 O. Bajjou, A. Bakour, M. Khenfouch, M. Baitoul, B. Mothudi, M. Maaza and E. Faulques, pH and concentration effect on the optical absorption properties of Sn(v) tetrakis (4-pirydyl) porphyrin functionalized graphene oxide, *J. Phys.: Conf. Ser.*, 2018, **984**, 012004.
25 M. Wormit, D. R. Rehn, P. H. P. Harbach, J. Wenzel, C. M. Krauter, E. Epifanovsky and A. Dreuw, Investigating excited electronic states using the algebraic diagrammatic construction (ADC) approach of the polarisation propagator, *Mol. Phys.*, 2014, **112**, 774–784.
26 P. H. P. Harbach, M. Wormit and A. Dreuw, The third-order algebraic diagrammatic construction method (ADC(3)) for the polarization propagator for closed-shell molecules: Efficient implementation and benchmarking, *J. Chem. Phys.*, 2014, **141**, 064113.
27 E. Runge and E. K. U. Gross, Density-Functional Theory for Time-Dependent Systems, *Phys. Rev. Lett.*, 1984, **52**, 997–1000.
28 *CRC handbook of chemistry and physics: a ready-reference book of chemical and physical data*, ed. W. M. Haynes and D. R. Lide, CRC Press, Boca Raton, Fla., 91st edn, 2010–2011, 2010.
29 Y. Shao, Z. Gan, E. Epifanovsky, A. T. B. Gilbert, M. Wormit, J. Kussmann, A. W. Lange, A. Behn, J. Deng, X. Feng, D. Ghosh, M. Goldey, P. R. Horn, L. D. Jacobson, I. Kaliman, R. Z. Khaliullin, T. Kuś, A. Landau, J. Liu, E. I. Proynov, Y. M. Rhee, R. M. Richard, M. A. Rohrdanz, R. P. Steele, E. J. Sundstrom, H. L. Woodcock, P. M. Zimmerman, D. Zuev, B. Albrecht, E. Alguire, B. Austin, G. J. O. Beran, Y. A. Bernard, E. Berquist, K. Brandhorst, K. B. Bravaya, S. T. Brown, D. Casanova, C.-M. Chang, Y. Chen, S. H. Chien, K. D. Closser, D. L. Crittenden, M. Diedenhofen, R. A. DiStasio, H. Do, A. D. Dutoi, R. G. Edgar, S. Fatehi, L. Fusti-Molnar, A. Ghysels, A. Golubeva-Zadorozhnaya, J. Gomes, M. W. D. Hanson-Heine, P. H. P. Harbach, A. W. Hauser, E. G. Hohenstein, Z. C. Holden, T.-C. Jagau, H. Ji, B. Kaduk, K. Khistyaev, J. Kim, J. Kim, R. A. King, P. Klunzinger, D. Kosenkov, T. Kowalczyk, C. M. Krauter, K. U. Lao, A. D. Laurent, K. V. Lawler, S. V. Levchenko, C. Y. Lin, F. Liu, E. Livshits, R. C. Lochan, A. Luenser, P. Manohar, S. F. Manzer, S.-P. Mao, N. Mardirossian, A. V. Marenich, S. A. Maurer, N. J. Mayhall, E. Neuscamman, C. M. Oana, R. Olivares-Amaya, D. P. O'Neill, J. A. Parkhill, T. M. Perrine, R. Peverati, A. Prociuk, D. R. Rehn, E. Rosta,

N. J. Russ, S. M. Sharada, S. Sharma, D. W. Small, A. Sodt, T. Stein, D. Stück, Y.-C. Su, A. J. W. Thom, T. Tsuchimochi, V. Vanovschi, L. Vogt, O. Vydrov, T. Wang, M. A. Watson, J. Wenzel, A. White, C. F. Williams, J. Yang, S. Yeganeh, S. R. Yost, Z.-Q. You, I. Y. Zhang, X. Zhang, Y. Zhao, B. R. Brooks, G. K. L. Chan, D. M. Chipman, C. J. Cramer, W. A. Goddard, M. S. Gordon, W. J. Hehre, A. Klamt, H. F. Schaefer, M. W. Schmidt, C. D. Sherrill, D. G. Truhlar, A. Warshel, X. Xu, A. Aspuru-Guzik, R. Baer, A. T. Bell, N. A. Besley, J.-D. Chai, A. Dreuw, B. D. Dunietz, T. R. Furlani, S. R. Gwaltney, C.-P. Hsu, Y. Jung, J. Kong, D. S. Lambrecht, W. Liang, C. Ochsenfeld, V. A. Rassolov, L. V. Slipchenko, J. E. Subotnik, T. Van Voorhis, J. M. Herbert, A. I. Krylov, P. M. W. Gill and M. Head-Gordon, Advances in molecular quantum chemistry contained in the Q-Chem 4 program package, *Mol. Phys.*, 2015, **113**, 184–215.

30 A. D. Becke, Density-functional thermochemistry. III. The role of exact exchange, *J. Chem. Phys.*, 1993, **98**, 5648–5652.

31 S. Grimme, Semiempirical GGA-type density functional constructed with a long-range dispersion correction, *J. Comput. Chem.*, 2006, **27**, 1787–1799.

32 P. Krishnakumar and D. K. Maity, Microhydration of a benzoic acid molecule and its dissociation, *New J. Chem.*, 2017, **41**, 7195–7202.

33 T. L. Eliason, D. K. Havey and V. Vaida, Gas phase infrared spectroscopic observation of the organic acid dimers $(CH_3(CH_2)_6COOH)_2$, $(CH_3(CH_2)_7COOH)_2$, and $(CH_3(CH_2)_8COOH)_2$, *Chem. Phys. Lett.*, 2005, **402**, 239–244.

34 J.-P. Cornard and C. Lapouge, Absorption Spectra of Caffeic Acid, Caffeate and Their 1 : 1 Complex with Al(III): Density Functional Theory and Time-Dependent Density Functional Theory Investigations, *J. Phys. Chem. A*, 2006, **110**, 7159–7166.

35 T. H. Dunning, Gaussian basis sets for use in correlated molecular calculations. I. The atoms boron through neon and hydrogen, *J. Chem. Phys.*, 1989, **90**, 1007–1023.

36 R. A. Kendall, T. H. Dunning and R. J. Harrison, Electron affinities of the first-row atoms revisited. Systematic basis sets and wave functions, *J. Chem. Phys.*, 1992, **96**, 6796–6806.

37 S. A. Epstein, D. Shemesh, V. T. Tran, S. A. Nizkorodov and R. B. Gerber, Absorption Spectra and Photolysis of Methyl Peroxide in Liquid and Frozen Water, *J. Phys. Chem. A*, 2012, **116**, 6068–6077.

38 D. Shemesh and R. B. Gerber, Molecular Dynamics of Photoinduced Reactions of Acrylic Acid: Products, Mechanisms, and Comparison with Experiment, *J. Phys. Chem. Lett.*, 2018, **9**, 527–533.

39 T. N. Truong and E. V. Stefanovich, A new method for incorporating solvent effect into the classical, ab initio molecular orbital and density functional theory frameworks for arbitrary shape cavity, *Chem. Phys. Lett.*, 1995, **240**, 253–260.

40 A. Bondi, van der Waals Volumes and Radii, *J. Phys. Chem.*, 1964, **68**, 441–451.

41 F. Plasser, B. Thomitzni, S. A. Bäppler, J. Wenzel, D. R. Rehn, M. Wormit and A. Dreuw, Statistical analysis of electronic excitation processes: Spatial location, compactness, charge transfer, and electron-hole correlation, *J. Comput. Chem.*, 2015, **36**, 1609–1620.

42 S. A. Mewes, F. Plasser, A. Krylov and A. Dreuw, Benchmarking Excited-State Calculations Using Exciton Properties, *J. Chem. Theory Comput.*, 2018, **14**, 710–725.

43 D. Marx, *Ab initio molecular dynamics: the virtual laboratory approach*, Wiley–VCH, Weinheim, 2007.

44 R. B. Gerber, D. Shemesh, M. E. Varner, J. Kalinowski and B. Hirshberg, Ab initio and semi-empirical Molecular Dynamics simulations of chemical reactions in isolated molecules and in clusters, *Phys. Chem. Chem. Phys.*, 2014, **16**, 9760–9775.

45 D. E. Romonosky, L. Q. Nguyen, D. Shemesh, T. B. Nguyen, S. A. Epstein, D. B. C. Martin, C. D. Vanderwal, R. B. Gerber and S. A. Nizkorodov, Absorption spectra and aqueous photochemistry of β-hydroxyalkyl nitrates of atmospheric interest, *Mol. Phys.*, 2015, **113**, 2179–2190.

46 E. Roth, A. Chakir and A. Ferhati, Study of a Benzoylperoxy Radical in the Gas Phase: Ultraviolet Spectrum and $C_6H_5C(O)O_2$ + HO_2 Reaction between 295 and 357 K, *J. Phys. Chem. A*, 2010, **114**, 10367–10379.

47 J. Towns, T. Cockerill, M. Dahan, I. Foster, K. Gaither, A. Grimshaw, V. Hazlewood, S. Lathrop, D. Lifka, G. D. Peterson, R. Roskies, J. R. Scott and N. Wilkens-Diehr, XSEDE: Accelerating Scientific Discovery, *Comput. Sci. Eng.*, 2014, **16**, 62–74.

